The EMBO Journal vol.13 no.20 pp.4938–4952, 1994

Fission yeast cut3 and cut14, members of a ubiquitous protein family, are required for chromosome condensation and segregation in mitosis

Yasushi Saka, Takashi Sutani, Yukiko Yamashita, Shigeaki Saitoh, Masahiro Takeuchi[1], Yukinobu Nakaseko and Mitsuhiro Yanagida

Department of Biophysics, Faculty of Science, Kyoto University, Kitashirakawa-Oiwake, Sakyo-ku, Kyoto 606, Japan
[1]Present address: Tularik Inc., 270 East Grand Avenue, South San Francisco, CA 94080, USA

Communicated by D.Glover

Fission yeast temperature-sensitive mutants *cut3-477* and *cut14-208* fail to condense chromosomes but small portions of the chromosomes can separate along the spindle during mitosis, producing ϕ-shaped chromosomes. Septation and cell division occur in the absence of normal nuclear division, causing the cut phenotype. Fluorescence *in situ* hybridization demonstrated that the contraction of the chromosome arm during mitosis was defective. Mutant chromosomes are apparently not rigid enough to be transported poleward by the spindle. Loss of the cut3 protein by gene disruption fails to maintain the nuclear chromatin architecture even in interphase. Both cut3 and cut14 proteins contain a putative nucleoside triphosphate (NTP)-binding domain and belong to the same ubiquitous protein family which includes the budding yeast Smc1 protein. The *cut3* mutant was suppressed by an increase in the *cut14*$^{+}$ gene dosage. The cut3 protein, having the highest similarity to the mouse protein, is localized in the nucleus throughout the cell cycle. Plasmids carrying the DNA topoisomerase I gene partly suppressed the temperature sensitive phenotype of *cut3-477*, suggesting that the cut3 protein might be involved in chromosome DNA topology.

Key words: chromosome condensation/chromosome segregation/DNA topoisomerase/fission yeast/mitosis

Introduction

Higher order chromosome structure alters strikingly during the cell cycle. As cells proceed into M-phase, interphase chromosomes are transformed into highly contracted metaphase chromosomes. Chromosomal regions on the nuclear envelope serve as foci for condensation and decondensation of the chromosomes in *Drosophila* embryonic nuclei (Hiraoka *et al.*, 1989). Higher eukaryotic chromosomes condense until they are only several micrometers long at mitotic metaphase, representing a 10 000-fold compaction of the length of naked DNA they contain. This chromosome condensation is implicated in ensuring correct sister chromatid separation into the daughter nuclei: condensation possibly enables the chromosomes to move without becoming entangled and makes them strong and compact enough to withstand the mechanical forces that are generated by the mitotic spindle. Upon completion of M-phase, chromosome structure reverts to the interphase state after decondensation. Molecular mechanisms for this cycle of chromosome condensation and decondensation in eukaryotic cells have been the subject of intensive investigations but are still poorly understood.

Chromosome condensation is a cell cycle regulated event (Murray and Hunt, 1993). This was shown by classical cell fusion experiments (Johnson and Rao, 1970; Rao and Johnson, 1970) which demonstrated that the chromosomes from G_1, S and G_2 cells displayed different degrees of premature condensation when these cells were fused to mitotic cells. In cell-free extracts, the chromosomes can be condensed if M-phase promoting factor is activated (Lohka and Maller, 1985; Newport and Spann, 1987; Murray and Kirschner, 1989). A variety of evidence suggests that chromatin is organized into loop domains in both interphase nuclei and mitotic chromosomes (reviewed by Gasser *et al.*, 1989). The chromosome scaffold fraction, which is resistant to solubilization after histone extraction and DNase treatment, contains proteins that may be required for anchoring these loops and for chromosome condensation in mitosis (Adolph *et al.*, 1977). One of the most abundant chromosome scaffold proteins is DNA topoisomerase II (topo II) (Earnshaw *et al.*, 1985; Gasser *et al.*, 1986). Using mitotic cell-free extracts, topo II was shown to be required for chromosome condensation (Wood and Earnshaw, 1990; Adachi *et al.*, 1991). A monoclonal antibody, MPM-2, which recognizes a class of mitosis-specific phosphoproteins (Davis *et al.*, 1983), was found to stain the central axis of condensed mitotic chromosomes formed *in vitro* (Hirano and Mitchison, 1991). These phosphoproteins might play a cell cycle regulated role in chromosome condensation.

A genetic approach to identification of genes that are responsible for chromosome condensation has been conducted using the fission yeast *Schizosaccharomyces pombe* as, in this yeast, chromosome compaction in the wild type and mutant cell cycles can be visualized by DAPI (4′,6-diamidino-2-phenylindole) staining, although the degree of compaction in wild type mitotic cells is less than that found in higher eukaryotes (Toda *et al.*, 1981; Uemura *et al.*, 1987a; Yanagida, 1990) and the compaction mechanisms may not be the same between fission yeast and higher eukaryotes. In metaphase-arrested mutant cells (Hirano *et al.*, 1988; Funabiki *et al.*, 1993), the arrangement of overcondensed chromosomes and the spindle within the nucleus is similar to that of higher eukaryotes; three condensed chromosomes are arranged to form a plate-like structure in the nucleus, and the short mitotic spindle runs through the central position of the plate (nuclear envelope breakdown does not take place in yeasts).

© Oxford University Press

Mutants in the topo II gene (*top2*$^{+}$) show defects in the final step of chromosome condensation (Uemura *et al.*, 1987a). In order to identify other temperature sensitive (ts) mutants which are defective in chromosome compaction, we searched for mutants which showed a phenotype similar to that found in ts and cold sensitive (cs) *top2* mutants (Uemura *et al.*, 1987a), that is, the so-called cut phenotype which allows cells to proceed to spindle formation and cytokinesis in the absence of normal nuclear division (Hirano *et al.*, 1986). In addition, the nuclear chromatin behavior in *top2* mutant cells at restrictive temperature is quite characteristic (Uemura and Yanagida, 1986): small portions of the chromosomal DNA were pulled and streaked poleward along the spindle, leaving the bulk of chromatin unseparated in the middle (Uemura and Yanagida, 1986; Funabiki *et al.*, 1993). The characteristic appearance of this ϕ-shaped nuclear chromatin prior to cytokinesis was a selection phenotype used for mutant screening.

Among 21 *cut* loci (Hirano *et al.*, 1986; Samejima *et al.*, 1993; our unpublished results), we have found that two *cut* mutations, namely *cut3-477* and *cut14-208*, produce phenotypes reminiscent of that of *top2* mutants. Here we report identification of their gene products, and provide evidence that both mutants are defective in mitotic chromosome condensation and segregation. The cut3 and cut14 proteins are similar to each other and belong to an apparently ubiquitous protein family which has recently been found, containing a nucleoside triphosphate (NTP)-binding consensus and including proteins from bacteria, budding yeast and mouse (Strunnikov *et al.*, 1993). The cut3 protein has the highest similarity to the mouse protein. Surprisingly, the protein is functionally related to topoisomerases. We propose that the degree of chromosomal DNA compaction is directly regulated by the cut3 and cut14 proteins through altering the topological states of chromosome DNAs in an NTP-dependent fashion.

Results

Isolation and nucleotide sequencing of the cut3^{+} and cut14^{+} genes

The *cut3*$^{+}$ gene was isolated by complementation of ts *cut3-477* (Hirano *et al.*, 1986), using an *S.pombe* genomic DNA library (Barbet *et al.*, 1992). A plasmid (pCUT3-23) was recovered from a Ts^{+} transformant and the region required for complementation was subcloned (Figure 1a). pCUT3-23 complemented both ts and null *cut3* mutants (construction of the null mutant is described below). Plasmid pYS353 containing the C-terminally truncated insert complemented ts but not null mutation.

To determine whether the cloned sequence came from the *cut3*$^{+}$ gene, the cloned DNA (2.7 kb *Pst*I fragment) was integrated with the *S.pombe ura4*$^{+}$ gene onto the chromosome of a host strain (*h*$^{-}$ *ura4*) by homologous recombination, and resulting stable Ura^{+} transformants obtained were analyzed by crossing with *cut3-477* and tetrad dissection. The marker was integrated at the *cut3* locus, establishing that the cloned DNA was derived from the *cut3*$^{+}$ gene. This was confirmed by complementation of both ts and null *cut3* by plasmid pST302 which contained the putative coding region under the *nmt1* promoter (Figure 1a; Maundrell, 1990).

The approximate location of the mutation site in *cut3-477* was determined by integration rescue (Figure 1a). Differently truncated *cut3* genes were integrated into the chromosome of *cut3-477*. Stable Ts^{+} transformants were obtained by pYS340 but not by pYS355, indicating that the mutation site was located in the C-terminal region.

Nucleotide sequencing indicated that the *cut3*$^{+}$ gene encodes a 1324 amino acid protein (predicted mol. wt, 150.6 kDa) as shown in Figure 1b. It was presumed that there were no introns. Database searching indicated that proteins with significant similarity exist in bacteria (*Mycoplasma hyorhinis* and *Rhodospirillum rubrum*), budding yeast and mouse (described below).

The *cut14*$^{+}$ gene was cloned by complementation of ts *cut14-208* mutant using two *S.pombe* genomic libraries (Beach and Nurse, 1981; Barbet *et al.*, 1992). Plasmids were recovered from plasmid-borne transformants and the region required for complementation was subcloned (Figure 2a). Verification of the cloned DNA derived from the *cut14*$^{+}$ gene was done by integrating the 1.8 kb *Hin*dIII fragment with the *LEU2* marker into the chromosome by homologous recombination, followed by tetrad dissection. The marker was integrated at the *cut14* locus, demonstrating that the cloned DNA contained the *cut14*$^{+}$ gene.

The *cut14*$^{+}$ gene encodes a 1172 amino acid protein (predicted mol. wt = 134.3 kDa; Figure 2b), 152 residues smaller than cut3. Database search showed that the predicted cut14 is similar to the set of proteins found when the search for proteins similar to cut3 was made. Direct comparison between cut3 and cut14 revealed that they were indeed similar (~20% overall identity; Figure 3).

Sequence comparison with budding yeast, bacteria and mouse proteins

Both cut3 and cut14 proteins are similar to the predicted amino acid sequences of the budding yeast Smc1 (Strunnikov *et al.*, 1993) and the *M.hyorhinis* P115 (Notamicola *et al.*, 1991). The overall sequence identity among these proteins was 22% between cut3 and Smc1, 18% between cut14 and Smc1, and 16% between p115 and cut3 or cut14. Sequence identity was relatively high in the N- and C-terminal regions, while being low in the central regions (Figure 3). The *SMC1* gene is required for minichromosome stability, while the function of the p115 protein is unknown except that it has an NTP-binding consensus sequence (indicated by the asterisks in Figure 3). These proteins are postulated to have the terminal globular domains connected to a rod-like central domain (Strunnikov *et al.*, 1993).

The highest score for amino acid identity was found between cut3 and the partial sequences in a mouse cDNA ORF (designated m. ORF in Figure 3; Varnum *et al.*, 1991) and Tsg73x (Höög, 1991). The identities of cut3 to m. ORF and Tsg73x are ~50%, while those of cut14 to the mouse sequences are much lower. The mouse ORF corresponds to the N-terminal cut3 sequence (aa 120–300). Tsg73x contains the sequence similar to the central region of cut3 (aa 620–700). The encoded protein function of the mouse cDNAs is unknown. The ubiquitous protein family hence appears to have different subclasses, and cut3 and the mouse protein may belong to the same subclass.

The N-terminal sequence surrounding the NTP-binding

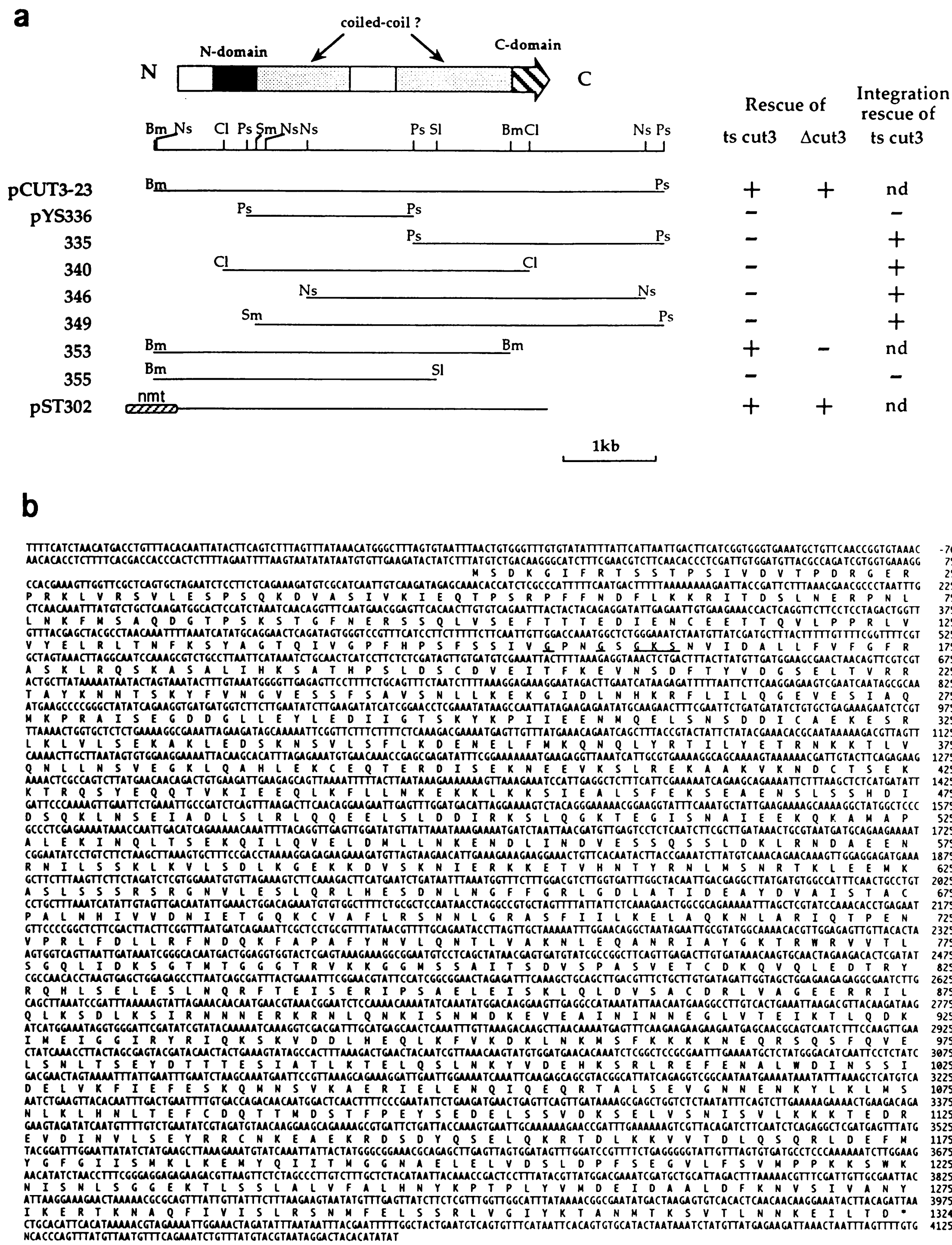

Fig. 1. Isolation and nucleotide sequencing of the *cut3*$^+$ gene. (**a**) Plasmid pCUT3-23 was obtained from a Ts$^+$ transformant, which complemented the ts phenotype of *cut3-477* mutant. This plasmid could also rescue the *cut3* null mutant (Δ*cut3*). Plasmids containing various parts of the insert in pCUT3-23 were employed for complementation and for the integration rescue of ts *cut3-477* mutant (+ indicates the rescue; nd, not determined). Plasmid pST302 contains the fission yeast inducible promoter *nmt1* (Maundrell, 1990) which is associated with the coding region of the *cut3*$^+$ gene. This plasmid rescued both ts and null mutations of *cut3* in the presence or the absence of thiamin (the *nmt1* promoter induces overexpression when thiamine is absent). The arrow indicates the coding region with the direction of transcription and the postulated functional subdomains. Some of the restriction sites are shown; Bm, *Bam*HI; Cl, *Cla*I; Ns, *Nsp*V; Ps, *Pst*I; Sl, *Sal*I; Sm, *Sma*I. (**b**) The nucleotide sequence of the cloned *cut3*$^+$ gene is shown with the predicted amino acid sequence. The predicted cut3 protein consists of 1324 amino acids. The residues for the NTP-binding consensus are underlined. The accession number of the sequence is D30788.

consensus is well conserved in cut3 and cut14 proteins (Figure 3). The C-terminal region containing the putative helix–loop–helix sequence (Strunnikov *et al.*, 1993) is also well preserved among the member proteins including the partial sequences of *Rhodospirillum rubrum* (Falk and Walker, 1988) and a budding yeast partial ORF (S.c. ORF; Shirahige *et al.*, 1993). The central domain is supposed to consist of coiled-coils with a non-coiled-coil subdomain

a

predicted ORF

Bg Bm RV Nh Bg Bm Nh Bm — Rescue of ts cut14

pYY1402 (Bm) +
1407 (Bm) -
1408 (Bm, Bm) -
1420 (RV, Bm) +
1409 (Bm, Bm) -
1411 (Bg, Bg, Bm) -
1412 (Nh) -
1413 (Nh, Nh) -

1kb

b

Fig. 2. Isolation and nucleotide sequencing of the *cut14*$^+$ gene. (**a**) Plasmid pYY1402 which complemented ts *cut14-208* was subcloned and the minimal insert in plasmid pYY1420 was obtained. + indicates complementation. The arrow indicates the coding region with the direction of transcription. Some of the restriction sites are shown; Bm, *Bam*HI; Bg, *Bgl*II; Nh, *Nhe*I; RV, *Eco*RV. (**b**) The nucleotide sequence of the cloned *cut14*$^+$ gene is shown with the predicted amino acid sequence. The predicted cut14 protein consists of 1172 amino acids. The residues for the NTP-binding consensus are underlined. The accession number of the sequence is D30787.

in the middle (Lupas *et al.*, 1991). The role of this central subdomain is unknown. These features are also conserved in cut3 and cut14 proteins.

Cell division arrest phenotype of cut3 and cut14 mutants

Previous studies showed that both *cut3-477* and *cut14-208* mutants at 36°C proceeded into cell division with abnormal nuclear division (Hirano *et al.*, 1986; Samejima *et al.*, 1993). These mutants formed normal colonies at 26°C. Both mutations were recessive.

The cell division phenotype in asynchronous culture was examined. Wild type, *cut3-477* and *cut14-208* grown in liquid culture at 26°C were shifted to 36°C. Cell division in *cut3* mutant continued for the next 6 h and then ceased, whereas *cut14* mutant was arrested earlier at 4 h (Figure 4a). The generation time of *cut3-477* at 36°C was identical to that of wild type (2.1 h), and thereby an

Fig. 3. Amino acid sequence comparison of cut3, cut14 and related proteins of bacteria, budding yeast and mouse. The predicted amino acid sequences of a mouse ORF (m. ORF) (Varnum *et al.*, 1991), fission yeast cut3, cut14, the budding yeast Smc1 (Strunnikov *et al.*, 1993), *Mycoplasma* p115 (Notamicola *et al.*, 1991), mouse Tsg73x (Höög, 1991), *Rhodospirillum rubrum* ORF (R.r. ORF) (Falk and Walker, 1988), *Saccharomyces cerevisiae* ORF (S.c. ORF) (Shirahige *et al.*, 1993) are aligned. Identical amino acid residues are boxed. The NTP-binding motif is indicated by asterisks.

~6-fold increase in cell number was obtained (cells divided by the cut phenotype were counted as two). Two or three rounds of cell division took place in *cut3*. In contrast, the cell number increase was only 2.4-fold in *cut14-208* at 36°C (the doubling time was ~3 h), indicating that *cut14* divided roughly once after the shift (Figure 4a).

Cell viability of *cut14* at 36°C rapidly decreased, whereas that of *cut3* remained high for the first 2 h and then decreased (Figure 4b). Consistently, the cut phenotype appeared in the first cell division for *cut14-208* (Samejima *et al.*, 1993) but in the second division for *cut3-477* mutant cells (described below). The difference was probably due to allele specific effects. The *cut14-208* mutation appeared to have a more severe effect on the *cut14*$^{+}$ gene product than the *cut3-477* mutation did on the *cut3*$^{+}$ gene product.

Abnormal nuclear division and the cut phenotype

Mutant *cut14-208* cells were incubated at 36°C for 2 h, fixed and stained with 4′,6-diamidino-2-phenylindole (DAPI) and anti-tubulin antibodies (Figure 4c). At this time point, cells in aberrant mitosis were more abundant than those in abnormal cytokinesis (Samejima *et al.*, 1993). Nuclear chromatin DNA was revealed by DAPI, while microtubules were visualized by monoclonal anti-tubulin antibody (Woods *et al.*, 1989).

The nuclear chromatin region in the *cut14-208* mutant cells was similar to the interphase structure except that a small part of it was pulled towards the opposite poles along the mitotic spindle which was fully extended (the middle panel of Figure 4c). This ϕ-shaped nuclear chromatin was peculiar, but reminiscent of the phenotype found in *top2* mutants at restrictive temperature (the top panel; Uemura and Yanagida, 1986; Funabiki *et al.*, 1993). As a control, wild type mitotic cells displaying the short mitotic spindle are shown (the bottom panel). The spindle apparatus was apparently normal in *cut14* mutant cells. It was formed during mitosis and fully elongated. The failure in sister chromatid separation in *cut14-208* mutant cells thus appeared to be due to a defect in the chromosomes rather than the spindle.

Synchronous culture analysis of cut3-477 mutant

The synchronous culture analysis was used to characterize the phenotype of *cut3-477*. Early G_2 cells collected by elutriation were cultured at 36°C. Aliquots of the culture were taken every 20 min and plated at 26°C to count viable cells. Cells were fixed for DAPI and anti-tubulin antibody staining (Figure 5). The *cut3-477* mutant cells lost viability at the rate of 20–30% after each cell division (panel a), and a severe mitotic phenotype was observed after the second division. Loss of cell viability occurred during mitosis and/or cytokinesis.

The cellular phenotypes at 36°C are schematized in Figure 5b. Type 1 cells are in interphase. Normal-looking cells containing divided nuclei without and with a septum (types 2 and 3 respectively) were abundant in the first division, but became nearly negligible in the second (Figure 5c). Abnormal type 4 cells containing divided nuclei connected to the chromatin fiber were present in

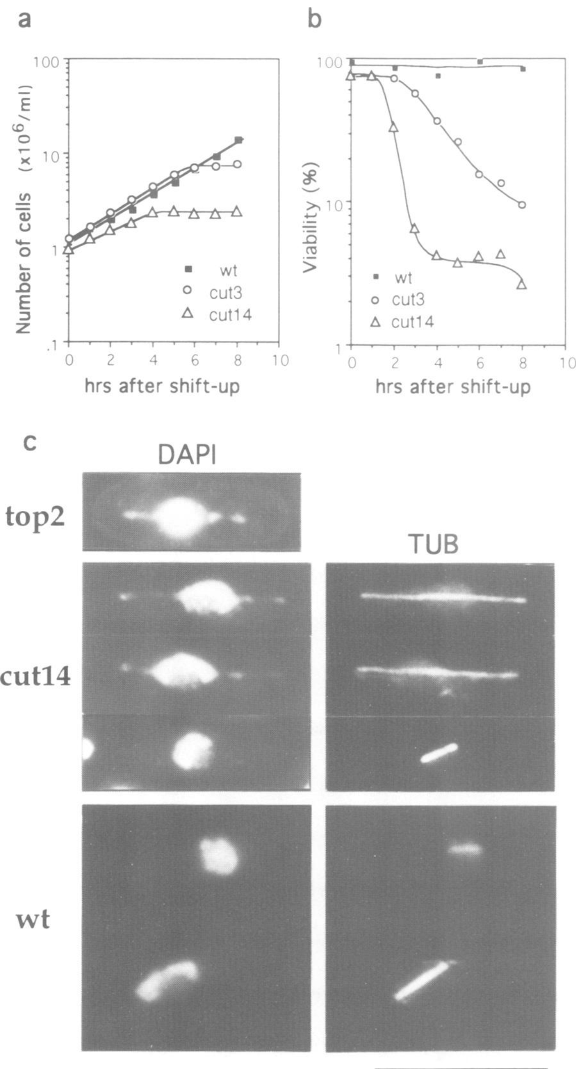

Fig. 4. Cell division phenotype of *cut3-477* and *cut14-208* at 36°C. (**a**) Wild type, *cut3-477* and *cut14-208* cells grown at 26°C were shifted to 36°C, and number of cells in each culture was measured. (**b**) The viability of wild type, *cut3-477* and *cut14-208* cells was measured by plating portions of the culture at 26°C. (**c**) Fluorescence micrographs of DAPI- and anti-tubulin-stained *cut14*, *top2* mutant and wild type cells. The *cut14* mutant cells were cultured at 36°C for 2 h, fixed and stained by DAPI and anti-tubulin antibody (TUB). The *top2* mutant cell was stained by DAPI after 2 h at 36°C as previously reported (Uemura and Yanagida, 1986). Small portions of DAPI-stained nuclear chromatin were pulled by the fully extended mitotic spindle toward the ends of the cell, but most of the chromatin remained in the middle of the cell without any sign of chromosome condensation. Cells in the bottom panel are wild type mitotic cells containing the short spindles. The bar indicates 10 μm.

both the first and the second divisions (Figure 5d). Cells displaying an extended area of nuclear chromatin without and with the septum (types 5 and 6 respectively) were frequent in the second mitosis. Cells producing the cut phenotype (type 7) appeared after the second division.

DAPI and anti-tubulin antibody staining of cells were performed at 120 and 220 min (in the first and second mitoses, respectively). Type 4 cells are shown in the upper panel of Figure 5e (120 min), while type 5 cells are seen in the lower panel (220 min). Cells containing short metaphase spindles are indicated by arrows.

Failure of chromosome arm contraction during mitosis

In neither *cut3* nor *cut14* mutant cells at restrictive temperature, have we observed any overcondensed chromosomes which are abundant in a number of mitotically arrested mutants such as *nda3* and *nuc2* (e.g. Hiraoka *et al.*, 1984; Hirano *et al.*, 1988). Chromosome condensation might be defective in *cut3* and *cut14* as these mutants, particularly *cut14-208*, have not revealed any obvious chromatin compaction in mitotic cells. The DAPI staining method, however, was not appropriate for comparing the decrease in chromatin compaction in wild type and mutant cells, although the method has been very useful for studying chromatin 'overcondensation' in mutant cells, which results in individual condensed chromosomes being visible. In wild type fission yeast cells, the degree of mitotic chromatin compaction is small when visualized by DAPI staining (Toda *et al.*, 1981). Mutants defective in chromosome condensation, if isolated, would reveal interphase-like nuclear chromatin during mitosis. It would be hard to distinguish between the wild type and the mutants by DAPI staining, since this reveals only the whole nuclear chromatin of the decondensed interphase nucleus. To monitor the degree of chromosome condensation, it would be most desirable to visualize the structure of one particular chromosome at any cell cycle stage.

To visualize an individual chromosome, we used fluorescence *in situ* hybridization (FISH), which has been applied in fission yeast (Uzawa and Yanagida, 1992; Funabiki *et al.*, 1993), using multiple hybridization probes to 'paint' a particular chromosome. Mixed hybridization probes consisting of 11 cosmids, all of which were derived from the left arm of chromosome II (Mizukami *et al.*, 1993), were prepared for painting (Figure 6, bottom panel). Antibodies against the spindle pole body (SPB) protein were simultaneously used to localize SPBs (Funabiki *et al.*, 1993). Their use enabled us to obtain information about the exact mitotic stages of individual cells and the positioning of the left arm of chromosome II in the nucleus relative to the SPBs at different cell cycle stages (Figures 6 and 7).

Wild type cells in interphase (WtIP) and mitosis (WtM) were first examined. The interphase cells contained a single SPB, while the mitotic cells contained two SPBs, which became further apart as mitosis progressed (Funabiki *et al.*, 1993). The spindle ran between the SPBs. In mitotic metaphase, the distance between the two SPBs is identical to the diameter of the spherical nucleus. During nuclear division equivalent to anaphase B, the dumbbell shaped nucleus had one SPB at each end.

In the interphase nucleus (WtIP), a rod-like chromosome arm was always observed by FISH (first column of Figure 6). One end of the rod is close to the SPB which is single in interphase (second column). This rod-like arm was confirmed by image reconstruction by through-focusing; the rod was more like a plate in the reconstructed images. DAPI staining which displayed the whole nuclear chromatin is in the third column, while the superimposed image of FISH, SPB and DAPI is depicted in the fourth column. Two more examples of wild type interphase cells visualized by FISH and anti-SPB antibodies are also shown in Figure 7.

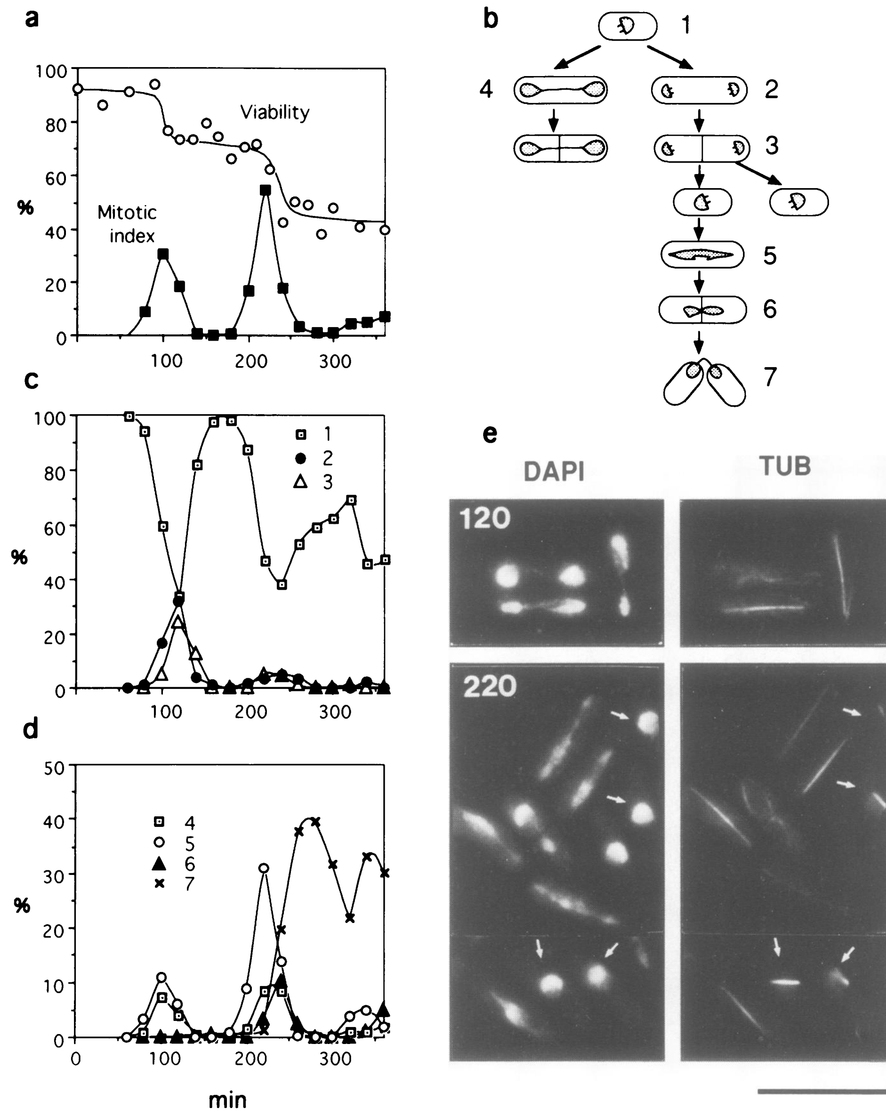

Fig. 5. Synchronous culture analysis of *cut3-477*. The *cut3-477* mutant cells grown at 26°C were run in an elutriator rotor, and small G_2 cells immediately after cell division were collected and incubated in rich YPD medium at 36°C. (**a**) Viability (open circles) and mitotic index (filled squares) after the temperature shift were estimated by plating at 26°C and microscopic examination of the nuclear spindle, respectively. (**b**) Schematic representation of *cut3-477* cells at 36°C. The seven classes of cells observed are shown. Type 1, interphase cells (judged by DAPI staining) containing the decondensed hemispherical nuclear chromatin (Toda *et al.*, 1991). Types 2 and 3, cells containing the divided nuclei without and with the septum, respectively. Types 4–7 show abnormal cell division phenotypes: type 4, cells containing the divided nuclei connected by thin chromatin fiber; types 5 and 6, cells displaying the extended nuclear chromatin without and with a septum, respectively; type 7, cells showing the cut phenotype. (**c**) The % frequency of type 1, 2 and 3 cells in the synchronous culture. (**d**) The % frequency of type 4–7 cells displaying aberrant mitosis or cytokinesis. (**e**) DAPI and anti-tubulin antibody staining of the *cut3-477* mutant cells. Cells were taken from the synchronous culture at 120 and 220 min, fixed and stained by DAPI and monoclonal anti-tubulin antibody (TUB). Upper panel, cells taken at 120 min. lower panel, cells taken at 220 min. Cells with short spindles are indicated by arrows. The bar indicates 10 μm.

Mid-mitotic wild type cells (WtM), which contained two SPBs close together, displayed a small spherical FISH signal. Two examples are shown in each of Figures 6 and 7. This contraction of the chromosome arm from interphase to mitosis was quite clear and highly reproducible in >100 mid-mitotic wild type cells examined. In the dividing daughter nuclei, condensed chromatids were still maintained (third row in WtM of Figure 6).

Two mutants, *cut3-477* and *cut14-208*, cultured at 36°C for 2–4 h were then examined (Figures 6 and 7). The rod-like FISH signals were always obtained from early to mid-mitotic cells of both (41 and 49 out of 50 *cut3* and *cut14* mutant cells examined, respectively), indicating that chromosome arm contraction was insufficient or did not occur in the mutant cells. Particularly, in *cut14-208* cells, the chromosome arm structure was nearly identical to that in interphase cells. In *cut3-477*, the chromosome arm seemed to be slightly contracted. In late mitotic cells, FISH signals were mostly present in the middle of the cell and small portions of the chromosomes were streaked along the spindle (third row of *cut3* and *cut14* in Figure 6). The sister arms were rarely separated in *cut14* (one out of 50 late mitotic cells), but were separated in nine out of 50 *cut3* mutant cells. We thus concluded that not only condensation but also sister chromatid separation were defective in the mutant cells. FISH using centromeric DNA sequences as probes (Funabiki *et al.*, 1993) demonstrated that centromere DNAs were separated and moved

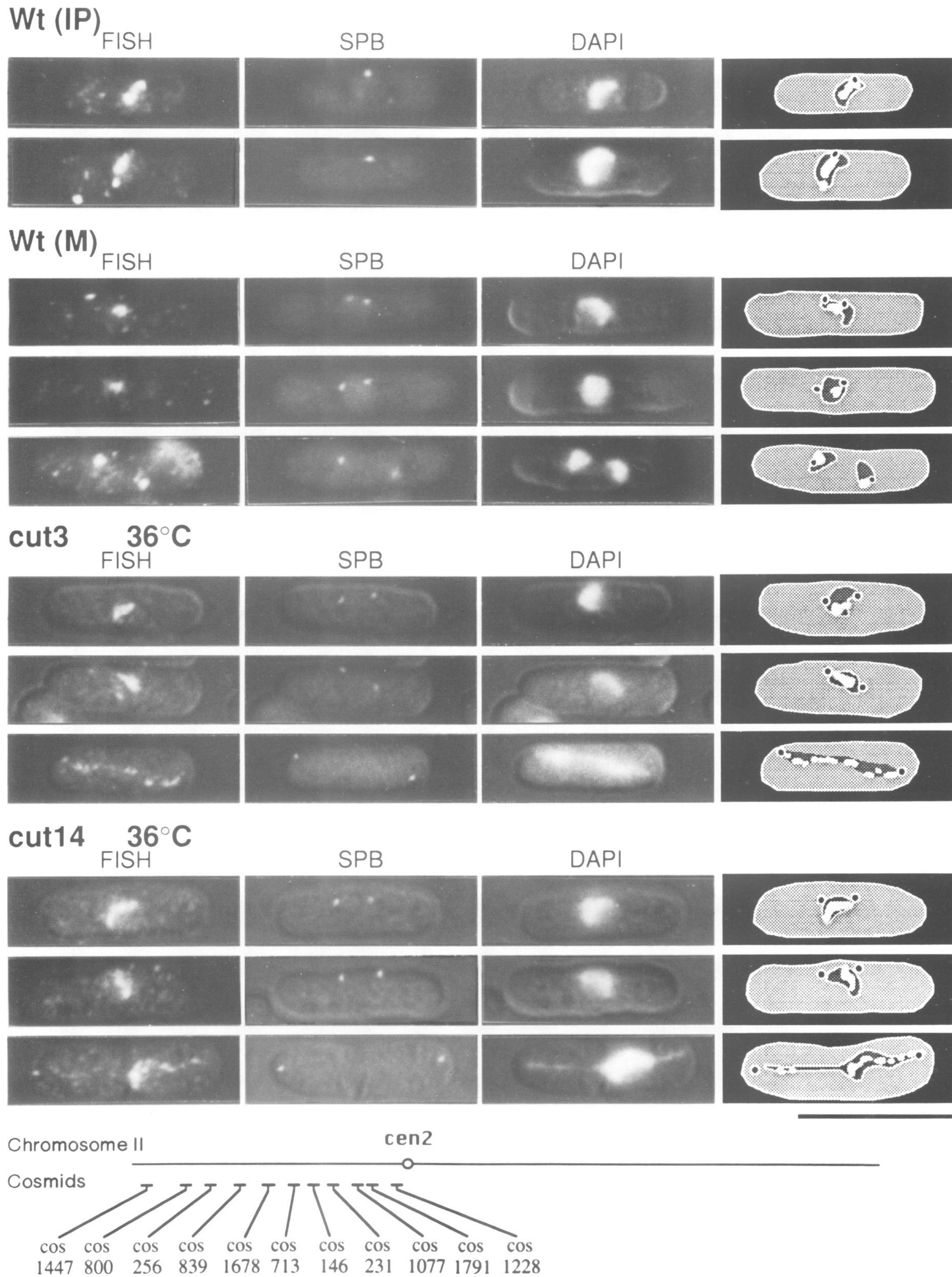

Fig. 6. Painting of the chromosome arm in *cut3-477* and *cut14-208* by FISH. Wild type, *cut3-477* and *cut14-208* cells cultured at 36°C for 4 and 2 h, respectively, were fixed, and the specimens for the FISH method were prepared. The probes for FISH consisted of mixed DNAs derived from 11 cosmids in the left arm of chromosome II (Mizukami *et al.*, 1993). Their approximate locations between the centromere and the left end are shown at the bottom. The SPBs were visualized using anti-sad1 antibodies and are shown in the second column (Funabiki *et al.*, 1993). In wild type interphase (Wt IP) and mitotic (Wt M) cells, the FISH signals which paint the left arm of chromosome II are shown on the left and are significantly different. DAPI-staining of nuclear chromatin is shown in the third column. Superimposed images of FISH, SPB and DAPI are depicted on the right. The bar indicates 10 μm.

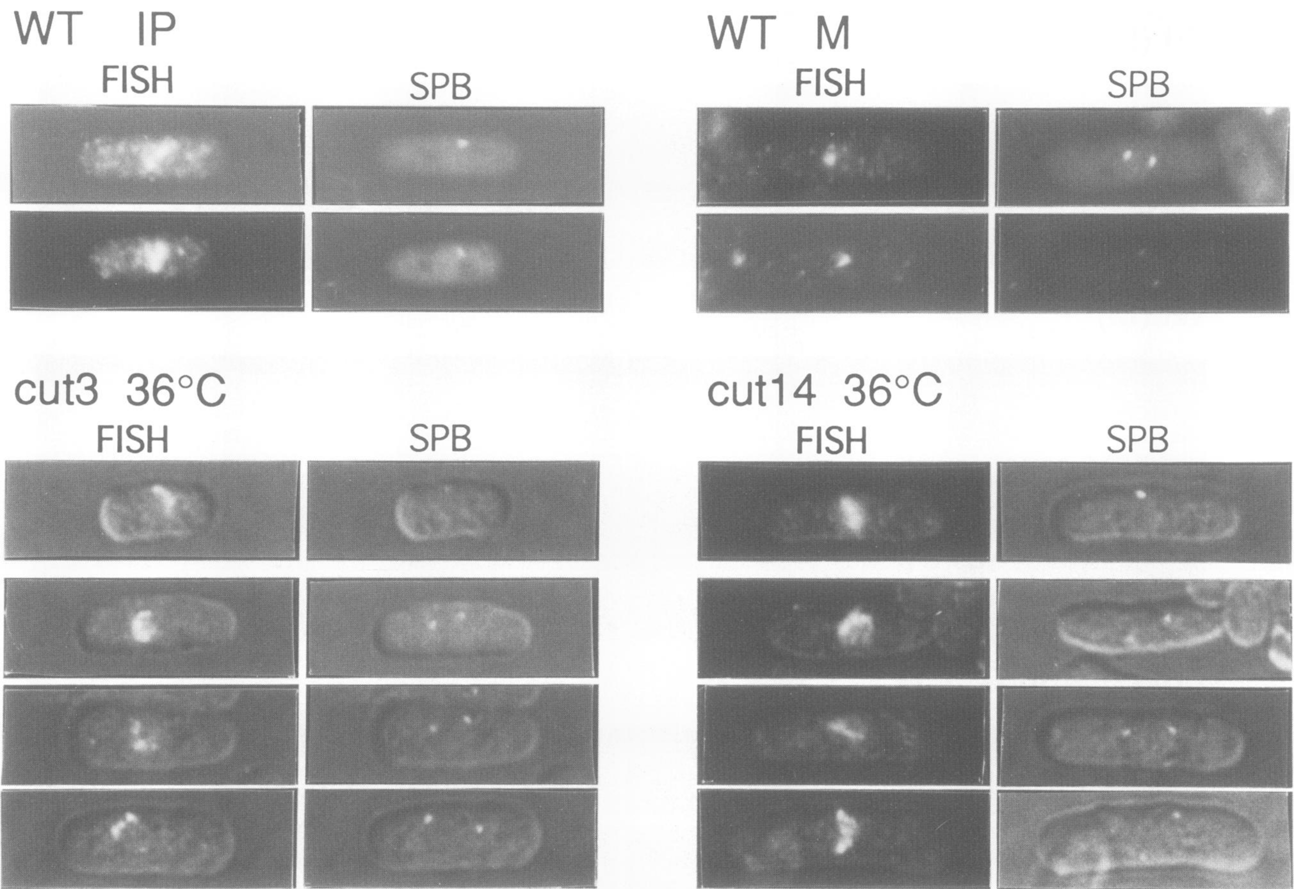

Fig. 7. Chromosome arm painting of wild type, *cut3* and *cut14* mutant cells by the FISH method. More examples of wild type, *cut3* and *cut14* mutant cells visualized by FISH and anti-SPB antibodies (the same procedure as in Figure 6) are shown. In the top panel, two wild type cells in interphase (left) and in mitosis (right) are shown. In the bottom panel, four cells (one interphase and three mitotic) each of *cut3* (left) and *cut14* (right) are shown. Chromosome arm contraction is defective in mutant cells. The bar indicates 10 μm.

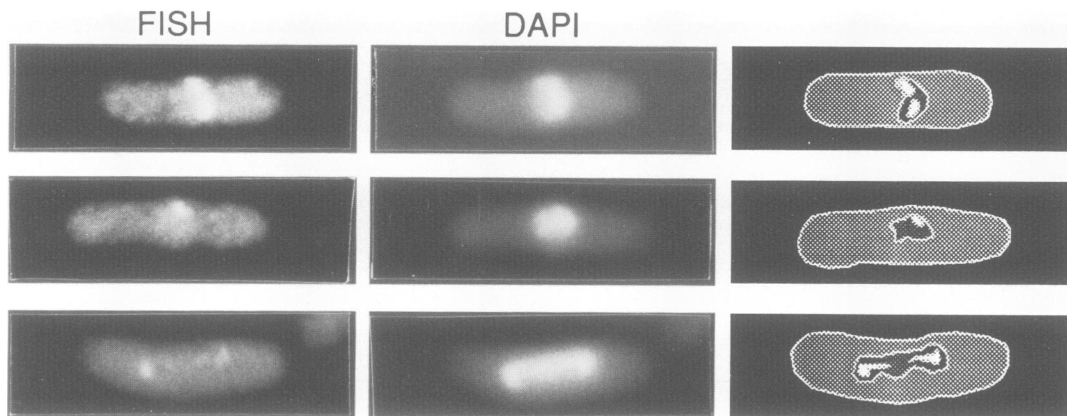

Fig. 8. Painting of the chromosome arm in *cut1* mutant cells by FISH. *cut1-206* cells were incubated at the restrictive temperature (36°C) for 1 h. Specimens for the FISH method were prepared as described in the previous figures. Interphase cell (top) showed the rod-like chromosome arm, while the normally contracted arm was seen in mid-mitotic cell (middle). In late mitosis, the arm was aberrantly separated as seen by DAPI staining of the whole chromatin. These micrographs showed that chromosome arm contraction was apparently normal but segregation was abnormal in *cut1* mutant cells. The bar indicates 10 μm.

to the opposite poles in *cut3* and *cut14* cells (data not shown).

cut1-206 mutant cells (Uzawa *et al.*, 1990) defective in chromosome segregation were employed as controls (Figure 8). The contracted mitotic chromosomes (Figure 8, second row) indistinguishable from that of wild type cells were made from the rod-like arm in interphase (first row). In late mitosis (third row), the arm was abnormally separated as if the whole nuclear chromatin had failed to segregate.

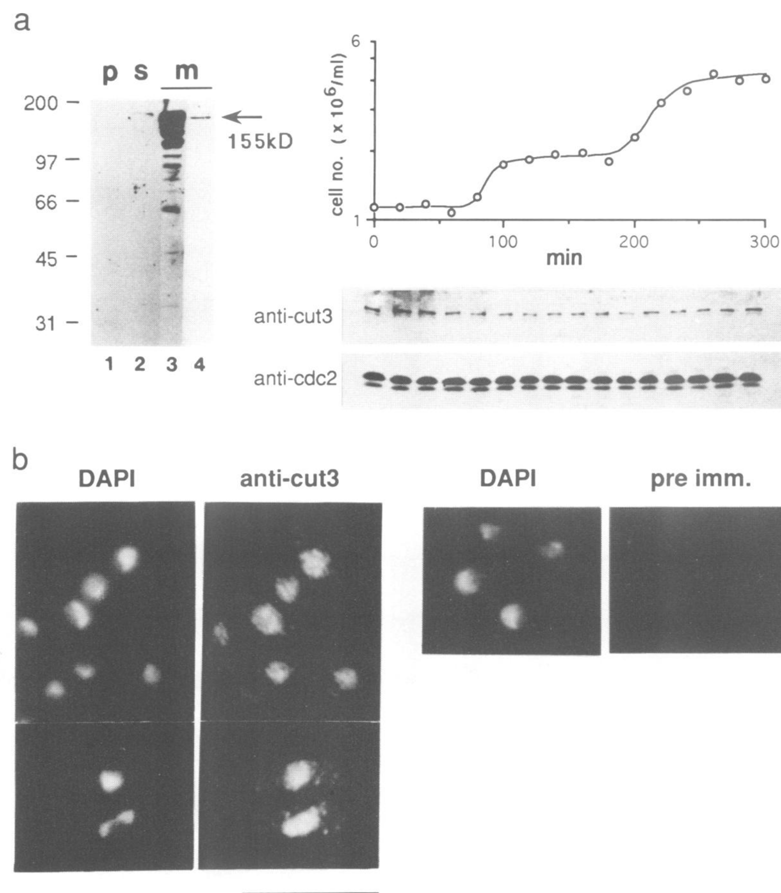

Fig. 9. Level of cut3 protein in the cell cycle and localization. (**a**) Left panel: immunoblot using antibodies against cut3. Extracts of wild type, wild type carrying multicopy plasmid with the *cut3*$^+$ gene were prepared and used for immunoblotting. Lane 1, wild type extracts detected by preimmune serum. Lane 2, wild type extracts detected by anti-cut3 antibodies. Lane 3, extracts of wild type carrying multicopy plasmid detected by anti-cut3 antibodies. Lane 4, a short exposure of lane 3. Right panel: synchronous culturing of wild type cells was performed at 33°C. Portions of the culture were taken at 20 min intervals and used for immunoblotting (shown at the bottom). The immunoblot pattern for the cdc2 protein is shown as control. The cell number was also measured at 20 min intervals. (**b**) Immunofluorescence micrographs of wild type cells stained by DAPI and anti-cut3 antibodies. Left, DAPI stain; right, affinity-purified anti-cut3 antibodies. The nucleus was stained by anti-cut3 antibodies. No nuclear signal was obtained by preimmune serum. The bar indicates 10 μm.

The same analysis was applied to *top2-191* mutant (data not shown). In 50 mid-mitotic cells examined, 20 did not show any compaction of the chromosome arm, while the remaining 30 cells displayed normal or significant contraction of the arm. Sister arms, however, were not separated in late mitotic cells of the *top2-191* mutant. The reduction of chromosome condensation was thus significant in *cut14*, *cut3* and *top2* mutants in that order.

Identification of the cut3 protein and its level in the cell cycle

To identify the product of *cut3*$^+$ gene, immunoblotting was performed using rabbit polyclonal antibodies made against the cut3 fusion protein (Figure 9a, left panel). Extracts of wild type cells (s) and wild type cells carrying multicopy plasmid with the *cut3*$^+$ gene (m) were prepared, run in electrophoresis and examined by immunoblotting. In wild type extracts (lane 2), a single 155 kDa polypeptide was seen, and its intensity was increased by the plasmid (lane 3). Short exposure of the high dosage extracts produced a band identical to that of wild type (lane 4). Preimmune serum showed no band (lane 1). Plasmids carrying the N-terminally truncated genes produced polypeptides reduced in size with expected mol. wts (data not shown). We hence concluded that the 155 kDa polypeptide was the product of the *cut3*$^+$ gene.

By employing anti-cut3 antibodies, the level of cut3 protein during the cell cycle was estimated in a synchronous culture (Figure 9a, right panel). The intensity of cut3 protein detected by immunoblotting did not change over two cycles of cell division.

Localization of the cut3 protein

Affinity-purified anti-cut3 antibodies were used for immunofluorescence microscopy (Materials and methods). Nuclear immunofluorescence was intense (Figure 9b, left panel). More cut3 protein is present in the chromatin region than in the non-chromosomal nuclear domain. Weak fluorescent signals were present in the cytoplasm. Preimmune serum gave very weak cytoplasmic signals but no nuclear signal (Figure 9b, right panel). Cells carrying a multicopy plasmid with the *cut3*$^+$ gene produced stronger nuclear fluorescence than did the wild type (data not shown).

Gene disruption phenotype of cut3

To determine whether the ts *cut3-477* phenotype is identical to that of *cut3* null, the *cut3*$^+$ gene was disrupted by

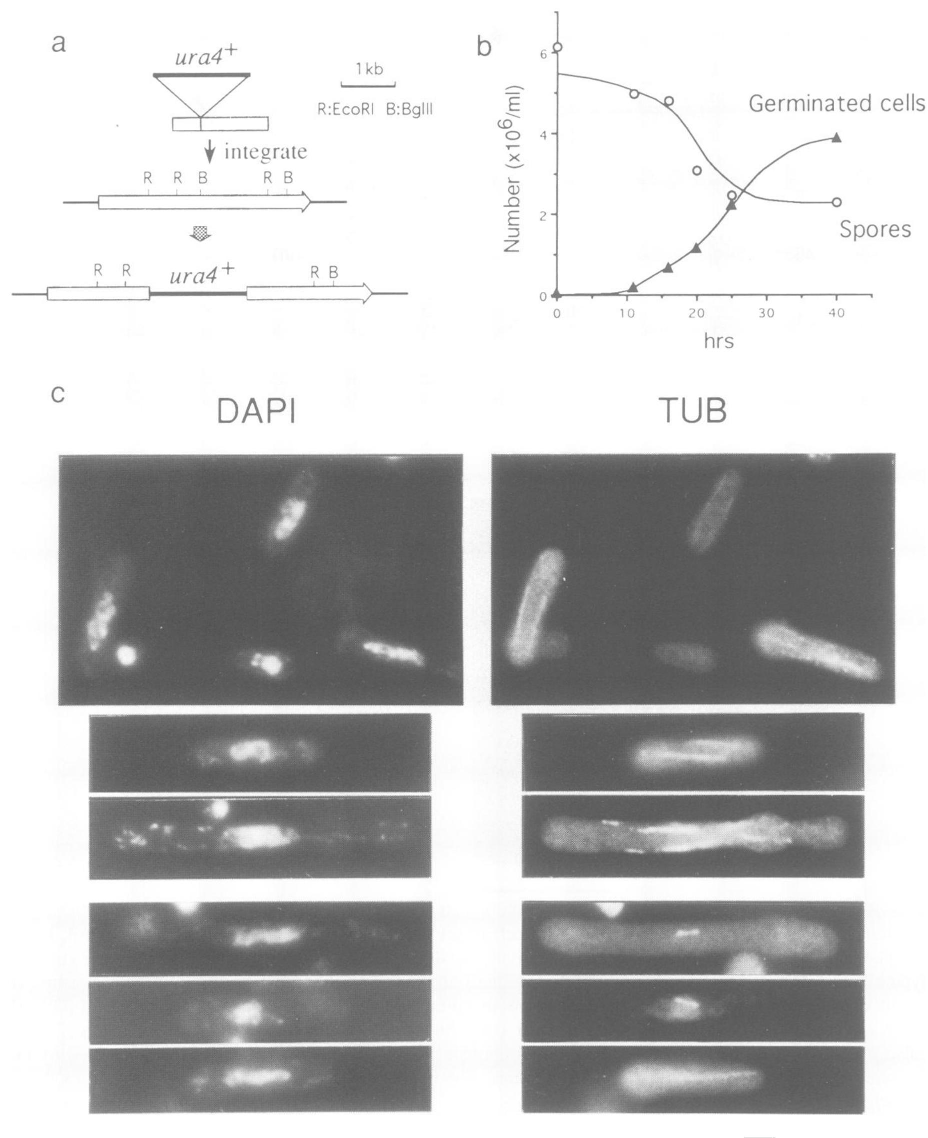

Fig. 10. The phenotype resulting from disruption of the *cut3*$^+$ gene. (**a**) The *S.pombe ura4*$^+$ gene was inserted at the *Bgl*II site of the *cut3*$^+$ gene, and the resulting interrupted gene was integrated into the chromosome. Verification of gene disruption was done using genomic Southern hybridization. Hybridization bands with the expected restriction sizes were obtained (not shown). (**b**) Heterozygous diploid cells were sporulated and then germinated in the absence of uracil. Under this condition, Ura$^-$ spores with the intact *cut3*$^+$ gene were unable to germinate. The numbers of germinated cells and remaining spores were counted under a light microscope. Most of the germinated cells were elongated but did not divide. Cells which had divided twice were negligible. (**c**) Germinated cells in the nutrient medium (lacking uracil) were stained by DAPI (left) and anti-tubulin antibody (right). Cells containing interphase microtubule arrays, which run from end to end in parallel, displayed swollen, extended fiber-like nuclear chromatin DNA. The cells containing the spindle also showed the swollen nuclear chromatin. Both interphase and mitotic cell types were abundantly present as well as cells showing the cut phenotype. The time course change after germination suggested that the interphase seemed to be greatly delayed. The bar indicates 10 μm.

one-step replacement and its phenotype was examined (Figure 10). The *cut3*$^+$ gene interrupted with the *ura4*$^+$ gene was integrated into one of the chromosomes in Ura$^-$ diploid cells by homologous recombination (a). Resulting Ura$^+$ heterozygous diploid cells were sporulated, and tetrads were dissected. In each tetrad there were two viable and two nonviable spores, and all the viable spores were Ura$^-$, demonstrating that the *cut3*$^+$ gene was essential for viability.

Heterozygous diploids were sporulated, and cells germinated from the gene-disrupted Ura$^+$ spores were counted in the liquid culture (panel b). The majority of germinated cells did not divide or divided only once. Cells were observed by DAPI combined with anti-tubulin antibody staining (panel c). Cells with interphase microtubules displayed extended nuclear chromatin with occasional fibrous appearance (left). Interphase nuclear chromatin seemed to be swollen. Mitotic cells with short spindles also contained swollen nuclear chromatin. These cells were highly abundant in the culture after 20 h at 33°C. Loss of the cut3 protein thus failed to maintain the nuclear chromatin architecture even in interphase. The cut3 protein thus may be required for higher-order chromatin organization throughout the cell cycle.

Interaction between cut3 and cut14

We found that multicopy plasmid carrying the *cut14*$^+$ gene weakly suppressed the ts phenotype of *cut3-477*.

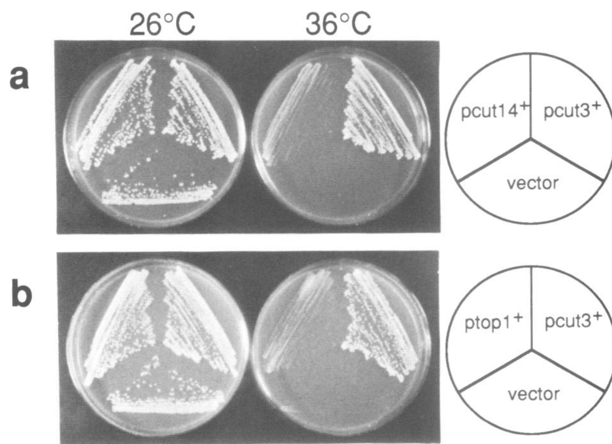

Fig. 11. Genetic interaction between the *cut3*$^+$, *cut14*$^+$ and *top1*$^+$ genes. (**a**) The ts *cut3-477* mutation was suppressed by a plasmid with the *cut14*$^+$ gene. *cut3* mutant cells carrying plasmid with the *cut14*$^+$ gene produced small colonies at 36°C, whereas cells carrying the vector plasmid did not. (**b**) The ts *cut3-477* mutant cells carrying plasmid with the *top1*$^+$ gene encoding topo I produced small colonies at 36°C.

Transformants produced small colonies at 36°C (Figure 11a), indicating that the two gene products interact directly or indirectly; they may have an overlapping function. However, transformants of *cut14-208* carrying plasmid with the *cut3*$^+$ gene failed to produce colonies at 36°C. Then, to examine which mutation was epistatic, the two strains were crossed and the double mutant *cut3-cut14* was constructed, which showed the *cut* phenotype after only 1 h at 36°C and showed complete loss of chromosome contraction at 36°C, more similar to single *cut14* than to *cut3*. The *cut14* mutation was thus epistatic to the *cut3* mutation. Plasmid carrying the budding yeast *SMC1* gene (a gift from Dr D.Koshland) suppressed neither *cut3-477* nor *cut14-208*.

Genetic interaction with DNA topoisomerases

Do cut3 and cut14 interact with topo II, which is known to be involved in chromosome compaction as well as segregation? In an initial attempt to address this question, we examined their genetic interaction using ts *top2-191* and cs *top2-250* (Uemura and Yanagida, 1984; Uemura *et al.*, 1987a). Double ts mutants, *cut3 top2* and *cut14 top2*, were constructed. The phenotype of *cut3 top2* at 36°C was similar to that of single ts *top2* mutant, while that of *cut14 top2* displayed a mixture of the phenotypes of the single mutants. Interestingly, the double mutant of ts *cut3-477* and cs *top2-250* was synthetically lethal; it did not form colonies at 30 or 33°C, while single mutants produced colonies at these temperatures. The cs topo II has a mutation in the ATP-binding domain and bound to and cleaved double-stranded DNA in the absence of ATP, whereas ts *top2-191* has a mutation site in the DNA binding domain and the ts topo II protein failed to associate with DNA at 36°C (Shiozaki and Yanagida, 1991).

Surprisingly, multicopy plasmid carrying the topo I gene (*top1*$^+$) partly suppressed the ts phenotype of the *cut3-477* mutant (Figure 11b). Transformants produced colonies at 36°C, although they were smaller than wild type. In contrast, multicopy plasmid with the *top2*$^+$ gene did not complement *cut3-477*. The *cut3*$^+$ gene appears to be functionally related to the *top1*$^+$ gene. The fission yeast *top1*$^+$ gene is not essential for cell viability and its multicopy plasmid does not suppress *top2* mutants: the *top1* null mutant cells grow normally at 26 and 36°C (Uemura and Yanagida, 1984; Uemura *et al.*, 1987b).

We constructed the double *cut3 top1* mutant by crossing, using *cut3-477* and *top1* deletion. It normally grew at 26°C but failed to produce colonies at 36°C. The phenotype of the *cut3 top1* mutant at 36°C is different from that of the single *cut3* mutant. The double mutant rarely (~5%) showed the cut phenotype after the shift to 36°C for 5 h. Cells often showed nuclear chromatin structure reminiscent of the 'ring' phenotype of the double mutant *top1 top2* (Uemura and Yanagida, 1984, 1986; Hirano *et al.*, 1989; Yanagida and Sternglanz, 1990). The cut phenotype was observed after 10 h.

Discussion

We report here that ts *cut3* and *cut14* mutant cells fail in chromosome condensation and sister chromatid separation during mitosis, but spindle elongation and cell division occur. The *cut3*$^+$ and *cut14*$^+$ genes were isolated and both found to belong to an apparently ubiquitous gene family which exists from bacteria to mouse and was first described in detail for the budding yeast *SMC1* gene (Strunnikov *et al.*, 1993). The *smc1* mutant is defective in chromosome disjunction, but it remains to be determined whether it is also defective in chromosome condensation. We show that the *cut3* mutant is partly suppressed by an elevated dosage of the *top1*$^+$ gene.

We provided evidence for the involvement of these mutations in chromosome condensation by the FISH method using mixed DNA probes from the left arm of chromosome II. FISH can provide information on individual chromosomes during the cell cycle when combined with anti-SPB antibody staining. Compaction of the chromosome arm was defective in *cut3-477* and *cut14-208* in early to mid-mitosis at the restrictive temperature. In wild type cells, the arm was rod-like in interphase and contracted into a sphere in mid-mitosis, and this arm contraction was defective in *cut3-477* and *cut14-208* at restrictive temperature. The change in the chromosome arm from interphase to mitosis was confirmed by computer-directed three-dimensional analysis of the images obtained by FISH (unpublished result in collaboration with Y.Chikashige and Y.Hiraoka). In mutant cells at late anaphase, most of the nuclear chromatin remained in the middle of cells, and only small portions were pulled out by the elongating spindle.

Spores of the *cut3* null mutant germinated but failed in the first cell division. Germinated cells displayed abnormally swollen nuclear chromatin in interphase and mitosis. Such extended chromatin regions were seen in most germinated cells, while control wild type germinated cells showed normal nuclear chromatin. This result suggested that the cut3 protein may be required for controlling interphase and mitotic chromatin organization. The ts cut3 protein probably retains part of the wild type protein function at the restrictive temperature. As the mutation site of *cut3-477* resides in the C-terminal domain, the N-terminal domain function might be exerted in the ts mutant cells at restrictive temperature.

The requirement of *cut3*$^+$ and *cut14*$^+$ in chromosome disjunction is probably directly related to their essential roles in chromosome condensation. Lack of chromosome condensation leads to the mutant chromosomes lacking the rigidity and structural integrity which are required for successful transportation towards the spindle poles. This notion is consistent with the phenotypes of *cut3* and *cut14*. The softened, uncondensed nuclear chromatin in mutant cells will not inhibit full elongation of the spindle but the spindle fails to transport the whole chromatid DNA as the chromatin is not sufficiently stiff. Only small portions of the nuclear chromatin are then pulled out and brought to the ends by the fully elongating spindle: the bulk of the chromatin body remains in the middle. The mutant chromosomes are not rigid enough to hold the entire structure under the pulling force generated by the mitotic spindle (Hays *et al.*, 1982). The present study provides evidence that chromosome condensation is a prerequisite for chromosome disjunction. Indeed, FISH showed that the centromeric DNA in *cut3* mutant cells was properly separated and moved to the spindle ends (data not shown), indicating that kinetochore function in anaphase A was normal, at least as far as the association of centromere DNA with kinetochore microtubules was concerned. Even a small spindle force would be sufficient to separate the centromere and neighboring chromatin DNAs, possibly allowing mutant cells to proceed with mitosis without being blocked at metaphase. The mutant phenotypes of *cut3* and *cut14* can thus be explained by the loss of normal chromosome condensation and rigidity in mitosis. Alternatively, the cut3 and cut14 proteins may be types of DNA topoisomerase essential for both condensation and segregation of chromosomes. Topo II was shown to be such an example by dissecting the steps of mitotic chromosome behavior before and after condensation (Uemura *et al.*, 1987). Such an approach has not been taken for *cut3* and *cut14* mutants, so the direct role of the cut3 and cut14 proteins in chromosome segregation remains to be determined. Only future study will clarify the role of these proteins in condensation and segregation of chromosomes.

The *cut3*$^+$ and *cut14*$^+$ genes may be directly required for chromosome disjunction as their amino acid sequences are similar to that of the budding yeast SMC1 protein whose mutant displayed defects in mitotic chromosome segregation and also mini-chromosome maintenance (Strunnikov *et al.*, 1993). We introduced fission yeast minichromosome Ch16 into *cut3-477*, but failed to find the high loss rate of Ch16 (unpublished result). DNA synthesis is not inhibited in *cut3-477*. The DNA contents of the mutant cells at restrictive temperature were estimated by FACS analysis. Only one peak for cells with a 2C DNA content was obtained in the mutant culture at 36°C (unpublished result). Other evidence for the normal progression of DNA synthesis in *cut3-477* was obtained by pulsed field gel electrophoresis of chromosome-sized DNA. Three regular chromosomal DNA bands were obtained in *cut3* mutant cells. In cells inhibited in S-phase by hydroxyurea, the chromosomal DNA bands disappeared (Hennessy *et al.*, 1991).

The cut3 and cut14 proteins are members of the new ubiquitous protein family (Strunnikov *et al.*, 1993) which contains the N-terminal NTP-binding consensus and the C-terminal putative helix–loop–helix domain. The central domain is presumed to be a coiled-coil-like structure with an intervening middle non-coiled-coil region. This overall feature, reminiscent of kinesin-like motor proteins and ATP-dependent DNA topoisomerases such as topo II and reverse gyrase, is conserved in cut3 and cut14. However, no strong sequence homology was found among these sequences. Of particular interest is the NTP-binding consensus; nuclear localization of cut3 suggests that the protein family may have the activity of DNA-dependent NTPase. By the polymerase chain reaction (PCR) using primers of the conserved regions of cut3 and mouse sequences, a *Xenopus* cDNA clone which encodes a polypeptide similar to the mouse and cut3 was obtained (Y.Adachi and M.Yanagida, unpublished result). Partial sequence of the *Xenopus* clone is highly similar (identity ≈90%) to the mouse ORF, suggesting high evolutional conservation in the subclass of the ubiquitous family.

A clue to understanding the molecular function of the cut3 protein came from a genetic experiment showing that the ts *cut3-477* mutant is suppressed by an elevated gene dosage of *top1*$^+$. Suppression is strong enough for *cut3* transformants to support cell division at 36°C. Another piece of evidence for genetic interaction between topo I and cut3 is that *cut3 top1* displays a phenotype strikingly different from that of single *cut3* and *top1* mutants. The *top1*$^+$ and *cut3*$^+$ genes might share a common function of maintaining higher order chromatin structure. The allele specific interaction between cs *top2* and ts *cut3* suggested that topo II might also be related to the function of the cut3 protein, but further study is needed to confirm such an interaction.

Eukaryotic topo I is known to relax both positive and negative supercoils through transient single strand breakage and rejoining (Cozzarelli and Wang, 1990). The enzyme does not require ATP. Eukaryotic topo II can relax supercoils, and decatenate and catenate circular DNAs through the transient double strand breakage and rejoining, but lacks the ability to supercoil the circular DNA. The enzyme does require ATP. The cut3 protein may be ATP-dependent type 1 DNA topoisomerase, but it does not resemble the sequence of reverse gyrase which is an example of such a case and makes positive supercoils (Kikuchi and Asai, 1984; Nakasu and Kikuchi, 1985; Confalonieri *et al.*, 1993). We propose that cut3 protein is involved in chromosome condensation by altering the degree of chromosomal DNA topology in an NTP-dependent fashion. They may not be DNA topoisomerases, but interact indirectly or directly with topo I and/or topo II. The NTP-binding site might serve to provide the chemical energy for structural change of chromosomes. Only future study will elucidate the molecular functions of this protein family, which will be of importance for understanding the mechanisms of chromosome condensation.

Hirano and Mitchison (1994) very recently found two *Xenopus* proteins present in chromosomes formed *in vitro*. The amino acid sequences of the cloned cDNA are very similar to those of the cut3 and cut14 proteins.

Materials and methods

Yeast strains, transformation and genetic methods

An *S.pombe* haploid wild type (972 h^-, 975 h^+), and ts *cut3-477* and *cut14-208* mutant strains were used (Hirano *et al.*, 1986; Samejima

et al., 1993). Topo I and II mutants, *top1* deletion and ts and cs *top2*, were previously described (Uemura and Yanagida, 1984; Uemura *et al.*, 1987a,b). Transformation of *S.pombe* was performed by the lithium method (Ito *et al.*, 1983). A host strain (*h⁻ ura4 cut3-477*) was employed for integration rescue by the cloned sequences. For gene disruption, the homozygous diploid (5A/1D, *h⁺/h⁻ leu1/leu1 his2/+ ade6-210/ade6-216 ura4/ura4*) was used. Wild type cells were grown to a density of 3×10^6 to 1×10^7 cells/ml at 33°C in rich YPD medium (1% yeast extract, 2% polypeptone, 2% glucose). Synthetic EMM2 medium was as described by Mitchison (1970). Two percent agar was added for plating. Temperature sensitive *cut3* and *cut14* strains used were grown in YPD to $1–5\times10^6$ cells/ml at 26°C, and then shifted to 36°C. Viability was estimated by plating the mutant cells at 26°C. The cell number was counted using a Micro cell counter (Sysmex).

Plasmids

An *S.pombe* genomic DNA library containing the *S.pombe ura4⁺* gene as the selection marker was a gift from Dr Antony M.Carr (Barbet *et al.*, 1992) and another library containing the *S.cerevisiae LEU2* gene was also used (Beach and Nurse, 1981). Plasmids recovered from Ts⁺ Ura⁺ or Ts⁺ Leu⁺ transformants obtained were subcloned into a minimal complementable genomic DNA. For integration of the cloned DNA onto the chromosome by one-step gene disruption (Rothstein, 1983), the integration vector pYC6 (Chikashige *et al.*, 1989) carrying the *S.pombe ura4⁺* gene as the marker was used. Plasmids carrying the fission yeast *top2⁺* or *top1⁺* gene were previously described (Uemura *et al.*, 1986, 1987b).

Isolation of the cut3⁺ and cut14⁺ genes

A host strain (*h⁺ ura4 cut3-477*) was employed for complementation using an *S.pombe* genomic DNA library previously described (Barbet *et al.*, 1992). The *S.pombe ura4⁺* gene was the marker for the vector. Transformed cells were incubated first at 26°C for 2 days, and then transferred to 36°C. Ura⁺Ts⁺ transformants were thus obtained, from which plasmid pCUT3-23 was recovered. The Ura⁺ and Ts⁺ markers cosegregated. pCUT3-23 fully rescued the ts phenotype of *cut3-477*. Procedures similar to those described above were used to isolate the *cut14⁺* gene by complementation of *cut14-208*. The *S.cerevisiae LEU2* (Beach and Nurse, 1981) and *ura4⁺* genes were employed as markers for the vector. Ts⁺Leu⁺ and Ts⁺Ura⁺ transformants were obtained using two genomic DNA libraries, and plasmids which fully rescued *cut14-208* were recovered. Nucleotide sequences of the isolated *cut3⁺* and *cut14⁺* genes were determined by the method described (Sanger *et al.*, 1977) by using a Taq DyeDeoxy™ Terminator Cycle Sequencing Kit and a 373A sequencer from Applied Biosystems (Foster City, CA).

Synchronous culture

The procedures for synchronous culture were previously described (Moreno *et al.*, 1989; Kinoshita *et al.*, 1990). *cut3-477* cells exponentially grown at 26°C were run in a Beckman elutriator rotor. Early G_2 cells (2×10^8 cells) were selected and incubated at 36°C in rich YPD medium. An aliquot of the culture was taken every 20 min, and the cell number and viable cell number were measured. By fluorescence microscopy of DAPI-stained cells, the frequencies of different cell types were estimated.

Fluorescence microscopy

DAPI staining of fission yeast cells was done as described (Adachi and Yanagida, 1989). Indirect immunofluorescence microscopy was performed by the method described (Hagan and Hyams, 1988) using anti-tubulin monoclonal antibodies (TAT-1; Woods *et al.*, 1989). *S.pombe* cells were fixed in culture medium containing 3.7% formaldehyde and 0.2% glutaraldehyde at 33°C for 1 h. The cells were digested with 0.6 mg/ml Zymolyase 100T (Seikagaku Corp., Tokyo), followed by permeabilization with 1% Triton X-100. For anti-cut3 staining, cells were fixed with 3.7% formaldehyde. Specimens for fluorescence microscopy were observed using a Zeiss Axiophot with a 100 W light source (HBO 100W/2). Photographs were taken using Kodak T-Max 400 or Ektachrome 400.

Preparation of antiserum and immunological methods

A fusion protein was made using the vector pGEX-KG (Guan and Dixon, 1991) and the resulting pGEXCUT3-3 plasmid containing a *Cla*I–*Eco*RI fragment (the *Cla*I site was treated by Klenow enzyme to make it blunt ended) was ligated into the *Sma*I and *Eco*RI sites of the vector. Glutathione S-transferase (GST) fusion protein was made in *Escherichia coli* MM294. Insoluble fusion protein was purified according to the procedures of Watt *et al.* (1985). The resulting polypeptide was injected into rabbits by the procedures described previously (Hirano *et al.*, 1988). Antigen was injected at 1 month intervals after the second injection, and sera were taken 10–14 days after injection. Antibodies were affinity-purified, first by incubating 10-fold diluted serum with nitrocellulose membrane blotted with GST in PBS/5% skim milk solution overnight and then by incubating with membrane blotted with the fusion protein antigen. Immunoblotting was performed according to Towbin *et al.* (1979). The second antibody used was horseradish peroxidase-labeled protein A (1/200 dilution) and detected by the ECL Western blotting system (Amersham). For immunofluorescence microscopy, anti-rabbit IgG antibody Cy3 (1/500 dilution; Chemicon International Inc.) was used as the second antibody.

Fluorescence in situ hybridization

The procedures for FISH in fission yeast were as described in Uzawa and Yanagida (1992) and Funabiki *et al.* (1993). In order to reveal chromosome II, 11 cosmids (Mizukami *et al.*, 1993) present in the left arm of chromosome II were employed as mixed probes for hybridization. The cosmids used are noted in the caption of Figure 6. These cosmid DNAs were independently prepared and then mixed for use.

Acknowledgements

We thank Drs A.Carr, K.Gull and D.Koshland for the gifts of DNA bank, anti-tubulin antibody and the SMC1 DNA clone, and T.Hirano and T.Mitchison for communicating information prior to publication. The work was supported by grants for the Specially Promoted Research and Human Genome Research from the Ministry of Education, Science and Culture of Japan. Y.S. is a Research Fellow of the Japan Society for the Promotion of Science.

References

Adachi,Y. and Yanagida,M. (1989) *J. Cell. Biol.*, **108**, 1195–1207.
Adachi,Y., Luke,M. and Laemmli,U.K. (1991) *Cell*, **64**, 137–148.
Adolph,K.W., Cheng,S.M., Paulson,J.R. and Laemmli,U.K. (1977) *Proc. Natl Acad. Sci. USA*, **11**, 4937–4941.
Barbet,N., Muriel,W.J. and Carr,A.M. (1992) *Gene*, **114**, 59–66.
Beach,D. and Nurse,P. (1981) *Nature*, **290**, 140–142.
Chikashige,Y., Kinoshita,N., Nakaseko,Y., Matsumoto,T., Murakami,S., Niwa,O. and Yanagida,M. (1989) *Cell*, **57**, 739–751.
Confalonieri,F., Elie,C., Nadal,M., Bouthier,C., Forterre de la Tour,P. and Duguet,M. (1993) *Proc. Natl Acad. Sci. USA*, **90**, 4753–4757.
Cozzarelli,N.R. and Wang,J.C. (eds) (1990) *DNA Topology and its Biological Effect*. Cold Spring Harbor Laboratory Press, Cold Spring Harbor, NY.
Davis,F.M., Tsao,T.Y., Fowler,S.K. and Rao,P.N. (1983) *Proc. Natl Acad. Sci. USA*, **80**, 2926–2930.
Earnshaw,W.C., Halligan,C.A., Cooke,C.A., Heck,M.S. and Liu,L.F. (1985) *J. Cell Biol.*, **100**, 1706–1715.
Falk,O. and Walker,J. (1988) *Biochem. J.*, **254**, 109–122.
Funabiki,H., Hagan,I., Uzawa,S. and Yanagida,M. (1993) *J. Cell Biol.*, **121**, 961–976.
Gasser,S.M., Laroche,T., Falquet,J., Boy de la Tour,E. and Laemmli,U.K. (1986) *J. Mol. Biol.*, **188**, 613–629.
Gasser,S.M., Amati,B.B., Cardenas,M.E. and Hofmann,J.F.-X. (1989) *Int. Rev. Cytol.*, **119**, 57–96.
Guan,K. and Dixon,J.E. (1991) *Anal. Biochem.*, **192**, 262–267.
Hagan,I. and Hyams,J.S. (1988) *J. Cell Sci.*, **89**, 343–357.
Hays,T.S., Wise,D. and Salmon,E.D. (1982) *J. Cell Biol.*, **93**, 374–382.
Hennessy,K.M., Lee,A., Chen,E. and Botstein,D. (1991) *Genes Dev.*, **5**, 958–969.
Hirano,T. and Mitchison,T.J. (1991) *J. Cell Biol.*, **115**, 1479–1489.
Hirano,T. and Mitchison,T.J. (1994) *Cell*, in press.
Hirano,T., Funahashi,S., Uemura,T. and Yanagida,M. (1986) *EMBO J.*, **5**, 2973–2979.
Hirano,T., Hiraoka,Y. and Yanagida,M. (1988) *J. Cell Biol.*, **106**, 1171–1183.
Hirano,T., Konoha,G., Toda,T. and Yanagida,M. (1989) *J. Cell Biol.*, **108**, 243–253.
Hiraoka,Y., Toda,T. and Yanagida,M. (1984) *Cell*, **39**, 349–358.
Hiraoka,Y., Minden,J.S., Swedlow,J.R., Sedat,J.W. and Agard,D.A. (1989) *Nature*, **342**, 293–296.
Höög,C. (1991) *Nucleic Acids Res.*, **19**, 6123–6127.
Ito,H., Fukuda,Y., Murata,K. and Kimura,A. (1983) *J. Bacteriol.*, **153**, 163–168.

Johnson,R.T. and Rao,P.N. (1970) *Nature*, **226**, 712–722.
Kikuchi,A. and Asai,K. (1984) *Nature*, **309**, 677–681.
Kinoshita,N., Ohkura,H. and Yanagida,M. (1990) *Cell*, **63**, 405–415.
Lohka,M.J. and Maller,J.L. (1985) *J. Cell Biol.*, **101**, 518–523.
Lupas,A., Van Dyke,M. and Stock,J. (1991) *Science*, **252**, 1162–1164.
Maundrell,K. (1990) *J. Biol. Chem.*, **265**, 10857–10864.
Mitchison,J.M. (1970) *Methods Cell Physiol.*, **4**, 131–165.
Mizukami,T. *et al.* (1993) *Cell*, **73**, 121–132.
Moreno,S., Klar,A. and Nurse,P. (1991) *Methods Enzymol.*, **56**, 795–823.
Murray,A.W. and Kirschner,M.W. (1989) *Nature*, **339**, 275–280.
Murray,A. and Hunt,T. (1993) *The Cell Cycle, an Introduction.* W.H.Freeman and Co., New York.
Nakasu,S. and Kikuchi,A. (1985) *EMBO J.*, **10**, 2705–2710.
Newport,J. and Spann,T. (1987) *Cell*, **48**, 219–230.
Notamicola,S., McIntosh,M. and Wise,K. (1991) *Gene*, **97**, 77–85.
Rao,P.N. and Johnson,R.T. (1970) *Nature*, **225**, 159–164.
Rothstein,R.J. (1983) *Methods Enzymol.*, **101**, 202–211.
Samejima,I., Matsumoto,T., Nakaseko,Y., Beach,D. and Yanagida,M. (1993) *J. Cell Sci.*, **105**, 135–143.
Sanger,F., Nicklen,S. and Coulson,A.R. (1977) *Proc. Natl Acad. Sci. USA*, **74**, 5463–5467.
Shiozaki,K. and Yanagida,M. (1991) *Mol. Cell. Biol.*, **11**, 6093–6102.
Shirahige,K., Iwasaki,T., Rushid,N., Ogasawara,N. and Yoshikawa,H. (1993) *Mol. Cell. Biol.*, **13**, 5043–5056.
Strunnikov,A.V., Larionov,V.L. and Koshland,D. (1993) *J. Cell Biol.*, **123**, 1635–1648.
Toda,T., Yamamoto,M. and Yanagida,M. (1981) *J. Cell Sci.*, **52**, 271–287.
Towbin,H., Staehelin,T. and Gordon,J. (1979) *Proc. Natl Acad. Sci. USA*, **76**, 4350–4354.
Uemura,T. and Yanagida,M. (1984) *EMBO J.*, **3**, 1737–1744.
Uemura,T. and Yanagida,M. (1986) *EMBO J.*, **5**, 1003–1010.
Uemura,T., Morikawa,K. and Yanagida,M. (1986) *EMBO J.*, **5**, 2355–2361.
Uemura,T., Ohkura,H., Adachi,Y., Morino,K., Shiozaki,K. and Yanagida,M. (1987a) *Cell*, **50**, 917–925.
Uemura,T., Morino,K., Uzawa,S., Shiozaki,K. and Yanagida,M. (1987b) *Nucleic Acids Res.*, **15**, 9727–9739.
Uzawa,S. and Yanagida,M. (1992) *J. Cell Sci.*, **101**, 267–275.
Uzawa,S., Samejima,I., Hirano,T. and Yanagida,M. (1990) *Cell*, **62**, 913–925.
Varnum,B., Ma,Q., Chi,T., Fletcher,B. and Herschman,H. (1991) *Mol. Cell. Biol.*, **11**, 1754–1758.
Watt,R.A., Shatzman,A.R. and Rosenberg,M. (1985) *Mol. Cell. Biol.*, **5**, 448–456.
Wood,E.R. and Earnshaw,W. (1990) *J. Cell Biol.*, **111**, 2839–2850.
Woods,A., Sherwin,T., Sasse,R., McRae,T.H., Baines,A.J. and Gull,K. (1989) *J. Cell Sci.*, **93**, 491–500.
Yanagida,M. (1990) *J. Cell. Sci.*, **96**, 1–3.
Yanagida,M. and Sternglanz,R. (1990) In Cozzarelli,N.R. and Wang,J.C. (eds), *DNA Topology and its Biological Effects*. Cold Spring Harbor Laboratory Press, Cold Spring Harbor, NY, pp. 299–320.

Received on June 22, 1994; revised on August 2, 1994

Note added in proof

Saitoh *et al.* [Saitoh,N., Goldberg,I., Wood,E.R. and Earnshaw,W.C. (1994) *J. Cell Biol.*, in press] recently identified ScII, an abundant chromosome scaffold protein, as a member of the family described in this paper.